STAR COUNTS AND VISUAL EXTINCTIONS IN DARK NEBULAE

R. L. DICKMAN

Physics Department, Columbia University, New York, New York 10027

Physics Department, Rensselaer Polytechnic Institute, Troy, New York 12181[a]

The Ivan A. Getting Laboratories, The Aerospace Corporation, Los Angeles, California 90009

Received 22 September 1977; revised 16 January 1978

ABSTRACT

Application of star count techniques to the determination of visual extinctions in compact, fairly high-extinction dark nebulae is discussed. Particular attention is devoted to the determination of visual extinctions for a cloud having a possibly anomalous ratio of total to selective extinction. The techniques discussed are illustrated in application at two colors to four well-known compact dust clouds or Bok globules: Barnard 92, B 133, B 134, and B 335. Minimum masses and lower limits to the central extinction of these objects are presented.

I. INTRODUCTION

The past few years have seen a resurgence of interest, particularly on the part of molecular radio astronomers, in the problem of determining visual extinctions A_V over wide spatial extents in interstellar dark clouds (Kutner 1973; Myers 1975; Encrenaz *et al.* 1975; Tucker *et al.* 1976; Dickman 1976, 1977). The reason for this renewed interest is basically simple. Interstellar dark nebulae which contain sufficient abundances of trace molecular species to be profitably studied by radio-frequency spectral line techniques, are usually objects possessing total visual extinctions $A_V \gtrsim 2$ mag (Dickman 1975, 1977). Such clouds consist predominantly of molecular rather than atomic hydrogen (Hollenbach *et al.* 1971), and since the light, homonuclear H_2 molecule totally lacks a radio signature, indirect methods must be employed to ascertain its abundance. The widespread constancy in the interstellar medium of the ratio of visual extinction to atomic hydrogen column density, first established by Lilley (1955) and more recently investigated by Jenkins and Savage (1974), provides the basic method needed in this context, particularly since fairly general theoretical arguments can be adduced for its extension and application to dark clouds in the modified form of a constant ratio of molecular hydrogen column density to visual extinction (Dickman 1977).

There are at least two important applications of such molecular hydrogen determinations. First, correlation studies of molecular column densities with visual extinction (Myers 1975; Encrenaz *et al.* 1975; Tucker *et al.* 1976; Dickman 1977) in principle allow one to determine molecular abundances relative to molecular hydrogen. These ratios are of fundamental importance in providing observational checks on theoretical models of dark cloud chemistry. Second, if the distance to a dark cloud for which an extinction map has been obtained is known, the total mass of the cloud can be estimated and the question of the cloud's future evolution addressed. This point was first recognized and exploited by Bok (1948, 1956; Bok *et al.* 1971) and has been treated more recently by Schmidt (1975) and Dickman (1976, 1978). Both the above applications require visual extinction determinations at fairly high spatial resolution.

This paper discusses in some detail one method for obtaining visual extinctions in dark clouds by means of star counts. This approach, which involves the counting of stars without division into apparent magnitude intervals, has been refined and vigorously pursued by Bok and co-workers (Bok 1956; Bok and Cordwell 1973) and is particularly well-suited for obtaining extinction maps of fairly compact, relatively high-extinction clouds of the type often of interest to contemporary radio astronomers. The approach adopted is an illustrative one, the various techniques being illustrated in application to the reduction of star counts made of four well-known compact dust clouds, or Bok globules: Barnard 92, B 133, B 134, and B 335. Photographic materials for the counts consisted of both Palomar Observatory Sky Survey (POS) plates from the collection at Kitt Peak National Observatory, and a variety of plates kindly provided by B. J. Bok. A summary of the source materials is given in Table I.

The basic method used in this work involves making counts of the total number of stars in each part of a cloud for which the value of extinction is to be obtained. A transparent rectilinear grid of "reseau" squares is placed upon the plate to be counted, and the total number of stars in each reseau element recorded. Generally speaking, plate scale and the necessity of obtaining sufficient spatial resolution of the cloud (cf. Sec. II) dictate the size of the reseau used. A rectilinear grid is of course not an *a priori* requirement—other reseau geometries, better suited to a particular source morphology may be used (cf. Trimble 1977), so long as the reseau topology is reasonably regular and is maintained uniformly over the entire cloud.

The statistical error expected with a count of N stars

[a] Present affiliation.

 0004-6256/78/8304-0363$00.90

TABLE I. Photographic source materials for star counts.

Object	Plate	Color/ wavelength[a]	Emulsion/ filter	Plates scale (arcsec/mm)	Reseau scale (arcsec)	Remarks
B 92	POS 810 E	Red 6500 Å	103a-E 2444	67	67	1
B 92	POS 810 O	Blue 4300 Å	103a-O None	67	67	1
B 133	Steward 1137	Red 6500 Å	098-02 None	10	50	2,3
B 133	POS 692 O	Blue 4300 Å	103a-O None	67	67	1
B 134	ITT 634	Far-red 7500 Å		10	50	4
B 134	POS 692 O	Blue 4300 Å	103a-O None	67	67	1
B 335	ITT 616	Far-red 7500 Å		10	50	4
B 335	POS 574 O	Blue 4300 Å	103a-O None	67	67	1

[a] Wavelength denotes approximate center-of-plate passband.
(1) Glass negative plate.
(2) Film positive. Observer—B. J. Bok.
(3) 098-02 has double-valued wavelength response; high in blue and red, low in green. Treated as red-sensitive plate.
(4) Plate obtained with 140-mm ITT image tube on Steward Observatory 90-in. reflector. Plate provided by B. J. Bok.

in a reseau grid element is $\sqrt{N}$ (Bok 1937). A brief discussion of the resulting uncertainty in derived visual extinctions is given in the Appendix. If extinctions obtained from a number of different plates with possibly different scales are to be compared (as done in Sec. II), additional imprecision may result because of reseau placement and alignment errors. In the examples used to illustrate this paper, computer-generated transparent overlays were utilized to minimize such errors.

Extinctions derived from the star counts in each reseau square are computed relative to a nearby region of sky which is presumed to be free of obscuration. Usually, one must therefore perform counts in such a reference field, and considerable care must be taken to insure that the chosen field is indeed unobscured; otherwise systematic errors in the extinctions obtained for the cloud will ensue (Dickman 1976). Reference field star counts were made in each color for the four sources listed in Table I.

Inasmuch as star counts will generally be made from photographic plates or prints having peak sensitivites at various different wavelengths, reduction of the raw count data comprising the number of stars in each reseau element falls naturally into two stages: (1) determination of the extinction A_λ at the plate wavelength λ, at each location in the cloud; (2) reduction of these extinctions to their visual ($V \cong 5500$ Å) equivalents, so that all extinction data may be treated on a common footing. Each of these procedures is discussed successively below.

II. REDUCTION TO A_λ

The extinction at wavelength λ at a position in a dark cloud may be defined in an operational sense as follows. Suppose that $N(m_\lambda)$, the number of stars per unit area of sky brighter than magnitude m_λ, is known for the region of the sky in which the cloud lies. If one counts the number of stars per unit area in a reference region (0) adjacent to the cloud and presumed free of obscuration, one may then assign a limiting magnitude m_λ (0) to these counts. If at a location (1) in the cloud one then repeats the counting procedure, a corresponding magnitude $m_\lambda(1) \leq m_\lambda(0)$ is obtained which reflects the smaller number of stars seen through the obscuring cloud. The extinction A_λ (1) at point (1) is then simply

$$A_\lambda(1) = m_\lambda(0) - m_\lambda(1) \text{ mag} \qquad (1)$$

Therefore, when values of the stellar surface density $N(m_\lambda)$ (usually given as a base-ten logarithm) versus m_λ are available, reduction of the star counts is straightforward.

The above argument implicitly requires that all stars counted in an obscured region of a cloud actually lie behind the cloud. If the presence of one or more foreground stars is suspected, confirmation of this can often be obtained by photometric observations of the stars, and the affected counts appropriately corrected. Following Bok and McCarthy (1974), the data in this work are analyzed assuming that no foreground stars are present.

The only available general stellar surface density tabulations are those of van Rhijn (1929), which give $\log(N)$ per degree of sky area as a function of old photographic magnitude (essentially equivalent to modern blue magnitude m_B, $B \cong 4300$ Å), for various values of (old) galactic coordinates l, b. In reducing counts made from blue-sensitive plates therefore, one may simply utilize the van Rhijn tables for the l and b nearest the cloud in question. Inasmuch as most modern blue-sensitive materials used for star counts can be expected to possess limiting magnitudes significantly higher than the upper end of the van Rhijn surface density tabulations ($m_B = 18$), it will usually be necessary to make a linear extrapolation of the van Rhijn sequence from its last two values at $m_B = 17, 18$, to obtain values of m_B from

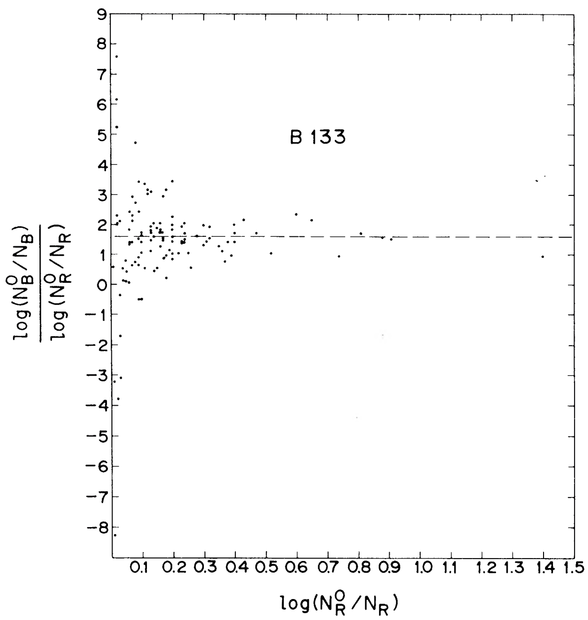

FIG. 1. Blue and red star count data computed for B 133 in order to test the assumption of a linear van Rhijn sequence in the red. If the assumption were strictly correct, in the absence of statistical fluctuations in the star counts, the data points would lie along the dotted line shown. See discussion in text.

counts of the reference field or low-extinction regions of the cloud. This is a relatively secure procedure since van Rhijn (1929) notes that the $\log N(m_B)$ sequences are linear to very good precision in the interval $15.5 \leq m_B \leq 18.5$.

An important property of the van Rhijn surface density functions is their near linearity for regions close to the galactic plane, where most dark clouds lie (Lynds 1962). That is, the relation

$$\log N(m_B) = a_B(l, b) + b_B(l, b) m_B \tag{2}$$

represents van Rhijn's data with a high degree of accuracy close to the galactic plane. Therefore, letting $n_B(1)$ denote the number of stars counted from a blue-sensitive plate in a reseau square where some extinction is present, and letting $n_B(0)$ denote the corresponding number of stars in an unobscured square of the same angular extent, (1) and (2) imply that the extinction in the blue through the cloud at position (1) is

$$A_B(1) = \frac{1}{b_B} \log \left[\frac{\alpha_r n_B(0)}{\alpha_r n_B(1)}\right] = \frac{1}{b_B} \log \left[\frac{n_B(0)}{n_B(1)}\right]. \tag{3}$$

Here α_r is the factor which normalizes the counts made over the reseau grid area to an area of 1 sq deg.

This relation forms the basis for interpreting star counts made at nonblue colors. Owing to the lack of independent general tabulations of stellar surface densities at such wavelengths, one must implicitly rely upon some extension of the blue van Rhijn sequences. Assuming (2) to be an adequate representation of the distribution of stars at λ_B, one may imagine the present red ($R \cong 6500$ Å) and far-red ($FR \cong 7500$ Å) distributions to be described by similar relations which may contain higher-order terms in m_R (for clarity, FR is suppressed as an index):

$$\log N(m_R) = a_R(l, b) + b_R(l, b)\, m_R + c_R(l, b)\, m_R^2 + \cdots. \tag{4}$$

A lowest-order approximation for red or far-red extinctions is therefore obtained by setting $c_R = 0$, $b_R = 0$, in which case one has analogous to (3):

$$A_R(1) = \frac{1}{b_B} \log \left[\frac{n_R(0)}{n_R(1)}\right]. \tag{5}$$

If the assumption of a linear van Rhijn sequence is rigorously correct, this procedure is identical to that advocated by Bok and Cordwell (1973) for the reduction of star counts at red colors, which involves counting the reference field in both blue and red colors and then scaling the red counts by the factor $[n_B(0)/n_R(0)]$. Its validity can be checked to a limited extent by noting that for red and far-red counts, one can consider the case $c_R = 0$, but with b_R distinct from b_B. If one then utilizes the fact that A_B and A_R are generally related by a simple multiplicative factor f_{BR} (Sec. III), at a given location (1) in a cloud one has

$$\frac{A_B(1)}{A_R(1)} = f_{BR} = \frac{b_R}{b_B} \left\{\frac{\log[n_B(0)/n_B(1)]}{\log[n_R(0)/n_R(1)]}\right\}, \tag{6}$$

where $f_{B\lambda} \cong 1.6$ and 2.0 for $\lambda = R$ and FR, respectively. Thus,

$$\frac{b_R}{b_B} = f_{BR} \left\{\frac{\log[n_R(0)/n_R(1)]}{\log[n_B(0)/n_B(1)]}\right\}. \tag{7}$$

If both blue and red counts are available for a source then a plot of the quantities in curly brackets versus $\log[n_R(0)/n_R(1)]$ (which, if $c_R = 0$, is proportional to the red extinction at position 1), can in principle serve not only to indicate the value of b_R/b_B, but, if a departure from a constant value is found, will signal the presence of a nonzero curvature term (c_R) in Eq. (4). This procedure was carried out for the sources listed in Table I. Because the blue and (far-) red star counts for each source generally involved different reseau scales, the grids of star numbers at each color were first made mutually compatible by scaling results on the finer mesh scale to those which would have been obtained with the coarser grid size; this was done by computer and unavoidably introduces a small amount of error because of the necessary assumption that stars are uniformly distributed within each small reseau element.

Results for the above procedure are shown in Figs. 1–4 for all locations in the sources where neither $n_B(1)$ nor $n_R(1)$ was zero. For each source the appropriate value of f_{BR} is indicated by a dashed line. The large scatter at

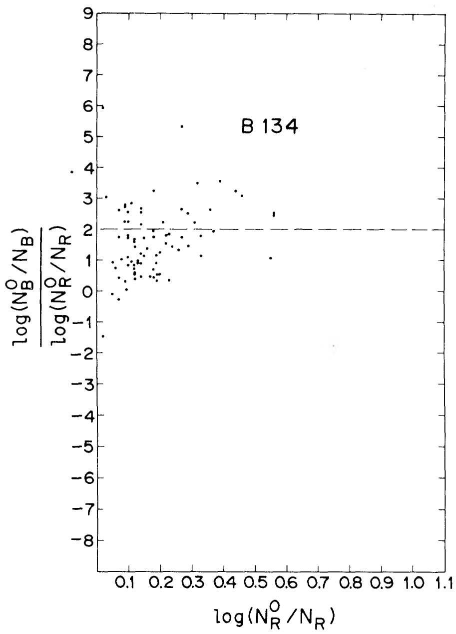

FIG. 2. Same as Fig. 1, but for blue and far-red counts of B 134.

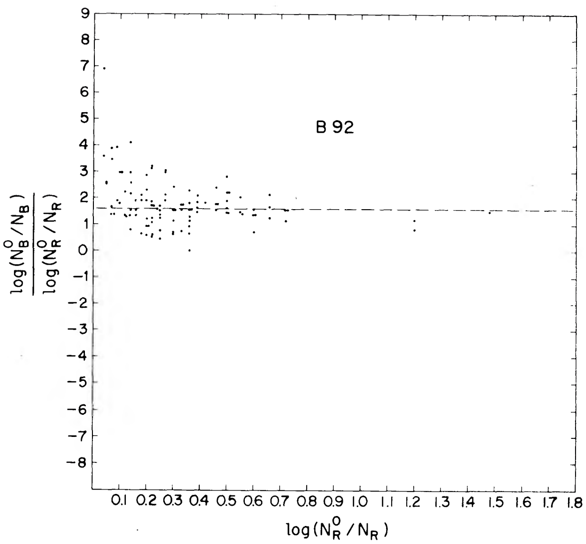

FIG. 4. Same as Fig. 1, but for blue and red star counts of B 92.

low values of the abscissae is due to statistical fluctuations in the star counts (see the Appendix) and the lack of symmetry about f_{BR} for B 134 and B 92 is attributable to slight reseau alignment discrepancies between the blue and red counts. The results embodied in Figs. 1–4 indicate that up to the comparatively low ($A_V \lesssim 4$ mag) extinctions probed in this fashion, use of the assumptions $b_R = b_B$ and $c_R = 0$ will lead to *at most* 15%–20% errors in derived values of red or far-red extinctions for these sources.

Therefore, while no rigorous substitute exists for tabulations analogous to those of van Rhijn at nonblue colors, the above results motivate the adoption of Eq. (5) for reducing star counts at these wavelengths to their corresponding extinction values. In doing so, a suitable value of the slope b_B is best determined by means of a least-squares fit to the van Rhijn sequence log $N(m_B)$ versus m_B for the l and b nearest to the source in question.

A final point to be mentioned here concerns the proper treatment of opaque core areas in dark clouds, in which no stars are seen in a number of reseau squares abutting one another. From the foregoing discussion it is evident that since the derived extinction depends upon the number of stars per unit area of sky, a lower limit to the extinction of an opaque cloud region must be determined by considering the *total* simply connected area of the cloud over which no stars are seen; one then assigns an upper limit of one counted star to such a region and normalizes to an area of 1 sq deg by the factor [Area (1°)/Area (core)]. It must be stressed that this is the only bias-free approach available in this context.

The above consideration emphasizes the necessity of choosing a reseau mesh fine enough to spatially resolve the most highly obscured parts of a cloud. If this is not done, it is easily shown that highly misleading results which grossly underestimate the minimum core extinction of the cloud will be obtained (Dickman 1976). Such a choice is obviously counterbalanced by the poorer count statistics obtained with a smaller reseau mesh, but of the two countervailing tendencies the necessity of a grid scale capable of resolving cloud structure is far more important (see Tucker *et al.* 1976 for further discussion of this point).

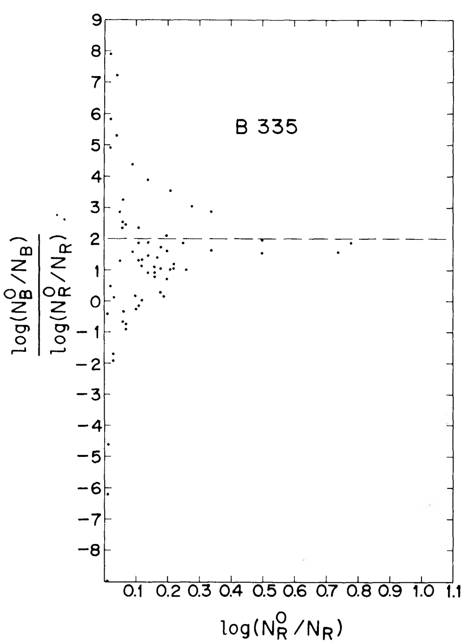

FIG. 3. Same as Fig. 1, but for blue and far-red counts of B 335.

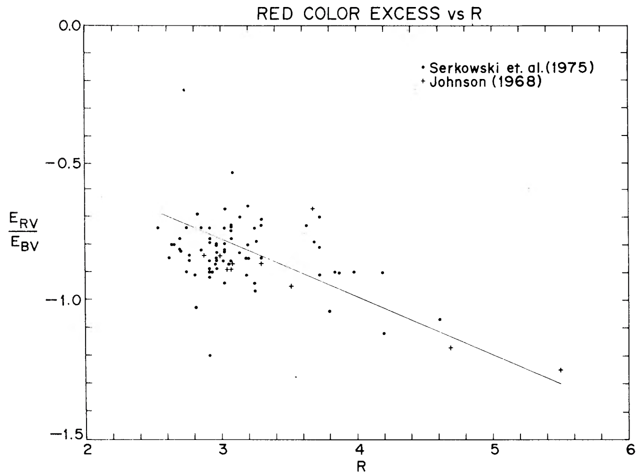

(a)

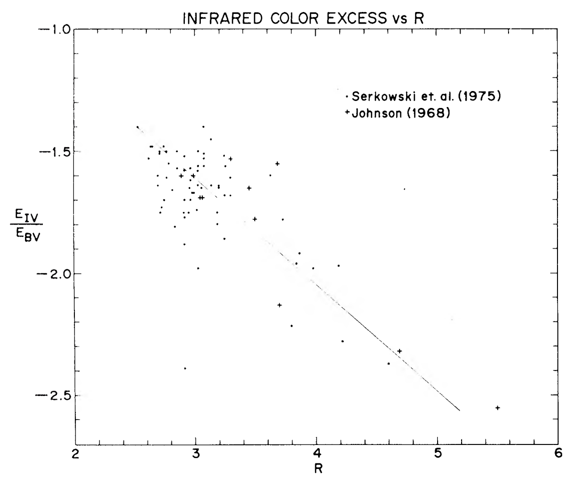

(b)

FIG. 5. (a) and (b) Observed dependence of reddening at I and R wavelengths upon the ratio of total to selective extinction, R. Plots are based upon the data of Johnson (1968) and Serkowski *et al.* (1975) and indicate that normalized color excess apparently decreases with increasing R, as shown roughly by the solid lines in each Figure. This suggests that even if a dark cloud possesses an anomalously large ratio of total to selective extinction, the conversion of blue and (far-) red extinctions to their visual equivalents as discussed in the text remains secure to within ~10%.

III. REDUCTION TO VISUAL EXTINCTIONS

In order to reduce values of extinction at some wavelength to their corresponding visual equivalents, the variation of extinction with wavelength (reddening law) must be known. With certain notable exceptions, an effectively "universal" reddening law (e.g., Whitford 1958; Wickramasinghe 1972) has been found to apply to much of the interstellar medium. In what follows we first consider the conversion of A_λ to A_V under the assumption that this law is generally applicable to dark nebulae. Thereafter, the effects of possible departures from a normal reddening law are assessed insofar as they directly concern the problem of determining visual extinctions. More general ramifications of possible reddening anomalies in dark clouds are discussed elsewhere (Dickman 1977).

Denoting the usual color excess by $E_{\lambda_1-\lambda_2} \equiv A_{\lambda_1} - A_{\lambda_2}$, the reddening law is conventionally expressed in terms of a function f of inverse wavelength λ^{-1} with the following normalization:

$$f(\lambda^{-1}) = E_{\lambda-V}/E_{B-V}. \qquad (8)$$

Thus one has in terms of R, the ratio of total to selective extinction,

$$f(0) = -R = -A_V/(A_B - A_V). \qquad (9)$$

Together (8) and (9) imply that

$$A_V = \left[\frac{R}{f(\lambda^{-1}) + R}\right] A_\lambda. \qquad (10)$$

Utilizing the normal interstellar reddening curve given by Bless and Savage (1972) with a value $R \cong 3.2$ (Harris 1973) therefore leads to the following relations between A_V and the various A_λ appropriate to star counts of the clouds in Table I:

$$A_V = 0.76\, A_B,$$
$$A_V = 1.21\, A_R, \qquad (11)$$
$$A_V = 1.48\, A_{FR}.$$

Deviations from the usual reddening law implicit in relations (11) have been suspected over the years for a number of specific locations in the sky (cf. Sherwood 1975 for a review). However, of those observations which have survived subsequent scrutiny, recent work (Carrasco *et al.* 1973, 1974; Strom *et al.* 1975; Vrba *et al.* 1975; see also Garrison 1977) which has disclosed possible evidence for increased values of the total to selective extinction ratio ($R \gtrsim 5$) in certain very dense interstellar clouds, is most directly relevant to the physical regime of dark nebulae. Generally (but see Baker 1976), these enhancements of R are attributed to a growth in the mean dust grain size in the clouds.

In the above work, R was determined by means of visual and infrared ($\lambda_K \sim 2.2\ \mu$) photometry of highly reddened early-type stars along the line of sight to the clouds. Values of increased R at high extinctions were found to correlate well with increased values of λ_{max}, the wavelength of maximum linear polarization observed for the stars. This is consistent with a grain-growth hypothesis since $\lambda_{max} \simeq 2\pi \times$ the mean grain radius (Greenberg 1968). More general work by Serkowski (1973; Serkowski *et al.* 1975) supports the existence of a widespread correlation of λ_{max} with R, and presents a number of additional cases of obscured stars for which the foreground material appears to possess an anomalously large ratio of total to selective extinction.

At present, it is uncertain whether or not enhanced

BARNARD 133

α_0 (1975) = $19^h\ 4^m\ 48.0^s$ δ_0 (1975) = -6° 57' 0.0"

ℓ_{II} = 28.4 b_{II} = -6.4

STEWARD PLATE 1137 PASSBAND CENTER = 6500 Å

RESEAU SCALE = 50.0"

								0.0	0.6	0.6	0.2	0.7	0.6	0.4	0.6	0.6	0.3									
								0.3	0.3	0.2	0.3	0.3	0.1	0.6	0.8	0.7	0.3									
								0.2	0.5	0.4	0.2	0.2	0.3	0.2	0.3	0.6	0.6									
								0.7	0.9	0.6	0.3	0.4	0.3	0.6	0.3	0.8	0.5									
								0.3	0.6	0.7	0.5	0.8	0.3	0.4	1.1	0.4	0.7									
								0.0	0.3	0.8	0.3	0.4	0.6	0.8	1.3	1.1	0.9									
								0.2	0.2	0.3	0.2	0.3	0.3	0.6	1.1	1.3	1.0									
						0.0	0.4	-0.0	0.1	0.3	0.3	0.5	0.2	0.7	1.3	1.0	0.5									
						0.1	0.1	0.0	0.2	0.1	0.6	0.2	0.3	0.4	1.4	1.3	0.6									
						0.2	-0.0	0.0	-0.1	0.2	0.4	0.7	0.5	0.8	1.5	1.3	0.7									
			0.1	0.1	0.2	-0.0	-0.1	-0.1	0.2	0.2	0.5	0.7	0.6	1.3	2.4	1.6	0.2	0.1	-0.0	-0.1	0.1	-0.0	0.1	0.2	-0.1	0.1
			0.0	0.0	0.3	0.1	0.0	0.1	0.4	0.2	0.2	0.5	1.4	3.4	7.6	0.9	0.4	-0.0	0.2	0.2	0.3	0.3	0.1	0.2	0.2	0.2
			0.0	0.1	0.4	0.0	0.1	0.0	0.7	0.3	0.7	1.4	1.8	4.8	7.6	1.1	0.5	0.0	-0.0	0.0	0.0	-0.0	-0.1	-0.0	0.3	-0.1
			0.2	0.2	0.3	0.2	0.2	0.3	0.3	1.7	1.6	2.8	4.8	7.6	3.9	0.3	0.5	0.1	0.2	0.1	-0.2	-0.1	0.2	0.3	-0.1	-0.0
			0.3	-0.1	0.2	0.0	0.3	0.1	1.4	3.4	2.6	4.8	3.9	7.6	2.4	1.0	0.2	0.3	-0.1	0.1	0.1	0.1	-0.1	0.6	-0.1	-0.0
			0.2	0.1	0.2	0.3	0.2	0.4	3.1	3.4	7.6	7.6	7.6	4.8	1.7	0.5	0.0	-0.0	0.1	0.2	0.0	0.2	0.5	0.2	0.1	-0.1
			0.6	0.5	0.3	0.6	0.4	1.9	4.8	7.6	7.6	4.8	7.6	2.6	1.1	0.8	0.7									
			0.6	0.7	0.4	0.2	0.6	3.9	4.8	3.9	2.4	2.6	2.6	0.9	0.8	0.7	0.3									
0.2	0.4	0.9	0.5	1.1	0.9	0.7	1.4	1.7	1.9	1.6	2.2	1.4	0.8	0.6	0.4	0.4	0.2									
0.0	0.4	0.3	0.6	0.4	0.2	0.2	0.5	0.9	0.9	0.2	0.5	0.1	0.2	0.1	-0.0	0.0	0.3									
0.2	-0.2	0.6	-0.1	0.1	-0.1	0.3	0.1	-0.1	0.2	0.0	0.0	-0.1	0.4	-0.1	0.2	0.2	0.2									
0.0	0.3	0.2	0.2	-0.0	-0.0	0.3	-0.0	-0.3	0.1	0.1	-0.0	0.2	0.3	-0.2	0.3	0.1	-0.1									
0.0	0.2	0.1	0.2	-0.1	-0.1							-0.2	-0.2	0.4												
0.2	-0.0	0.2	-0.1	0.0	0.2							-0.0	-0.1	-0.1												
-0.2	0.2	0.1	-0.0	0.6	0.2							-0.1	0.2	0.2												

FIG. 6. Visual extinction map of B 133 made from the red-sensitive plate listed in Table I. The reseau square centered at the coordinates given at the top of the map has been boxed. Lower limits to A_V are underlined.

values of R can be expected to occur in the dark clouds of moderate mass and density which are typically amenable to star count studies. Direct observational evidence is sparse (Carrasco *et al.* 1974; Fitzgerald *et al.* 1976) and there are theoretical difficulties with interpretations of enhanced R values which rest upon a grain-growth mechanism (Dickman 1977). However, one may approximately assess the effect which an anomalously high ratio of total to selective extinction, if present in a dark cloud, will have upon the reduction of red or far-red extinctions.

Photometric data of Serkowski *et al.* (1975) and Johnson (1968) have been utilized to construct values of $f(\lambda^{-1})$ for red and near-infrared wavelengths ($I \cong$ 8500 Å). These have been plotted against the ratio of total to selective extinction in Figs. 5(a) and 5(b). Where possible, R was determined as a mean of polarization value $R_{\text{pol}} = 5.5\ \lambda_{\max}$ (Serkowski *et al.* 9175) and photometric value $R_{\text{ph}} = 1.1\ (E_{V\text{-}K}/E_{B\text{-}V})$ (Carrasco *et al.* 1973). In some cases however, only one of these values could be used. Inspection of Figs. 5(a) and 5(b) reveals an approximately linear drop in both $f(\lambda_R{}^{-1})$ and $f(\lambda_I{}^{-1})$ as R increases, these variations being roughly indicated by the slanted lines in each figure. The decrease in the two f values with increasing R then suggests that insofar as these data can be considered to be generally applicable to dark clouds, the conversion factors (11) remain secure to within ~10% despite the apparent enhancement of the ratio of total to selective extinction.

IV. VISUAL EXTINCTIONS FOR CLOUDS

Maps of visual extinctions for the sources listed in Table I have been obtained by application of the techniques discussed in Secs. II and III, and are shown in Figs. 6–13. In each case the reseau square centered at the cloud coordinates given at the top of each figure is boxed. Lower limits to the extinction through any opaque areas in the sources are underlined. In most cases, a field considerably larger than the extent of each cloud was counted, so that a large part of each map just reflects expected statistical fluctuations about the value A_V = 0 (Appendix).

Generally, the agreement between the maps made from blue- and red-sensitive plates for each source is excellent. In making such a comparison, one must of course allow for the quantization of star numbers (and therefore extinctions) produced by the reseau, and also for the fact that the red-sensitive plates penetrate the globules far better than their blue counterparts; this improves counting statistics and allows a higher limit to the central extinction to be set. It is evident that given the limiting magnitudes of the photographic materials in the present study, increasing the reseau resolution would be of only marginal usefulness, since statistical fluctuations would then begin to dominate derived extinctions. On the other hand, averaging extinction values obtained for these clouds over a coarser resolution scale, as was done by Dickman (1977) for a comparison of A_V

BARNARD 133

α_0 (1975) = $19^h\ 4^m\ 48.0^s$ δ_0 (1975) = $-6°\ 57'\ 0.0''$

ℓ_{II} = 28.4 b_{II} = −6.4

POS PLATE 0692 PASSBAND CENTER = 4280 Å

RESEAU SCALE = 66.7″

					-0.1	0.4	0.7	0.4	0.3	1.0	0.4	0.4
					0.6	0.6	0.5	0.4	0.6	0.6	0.6	0.6
					0.7	0.4	0.5	0.9	0.3	0.8	0.7	0.2
				0.0	0.2	0.4	0.3	0.8	1.4	2.7	1.1	0.6
				0.1	-0.2	0.1	0.1	0.8	1.1	1.4	0.9	0.5
				0.2	0.2	-0.0	0.6	0.6	0.1	1.6	0.6	0.2
				0.2	0.0	0.3	0.6	0.9	1.2	2.7	0.7	0.2
				0.2	0.1	0.2	0.7	1.2	2.7	2.7	0.9	0.2
				0.0	0.3	0.5	1.6	2.7	4.7	2.7	0.8	0.3
				0.1	0.5	1.4	2.7	2.7	4.7	1.1	0.3	0.4
0.2	0.1	0.0	-0.1	0.2	1.1	4.7	4.7	4.7	4.7	1.4	0.4	0.5
0.2	0.6	0.3	0.1	0.3	4.7	4.7	4.7	4.7	2.1	1.1	1.0	0.5
0.2	0.5	0.9	0.6	1.8	4.7	4.7	4.7	2.7	0.9	0.6	0.2	0.4
0.3	0.6	0.4	0.6	0.7	1.0	0.8	0.4	0.3	0.3	0.1	0.2	0.2
0.2	0.1	0.1	0.0	0.1	0.2	0.3	-0.0	0.0	-0.1	0.2	0.0	-0.1
0.4	0.1	0.2	0.2	-0.0	0.2	-0.0	0.1	0.3	0.0			
							-0.1	0.0	0.0			
							0.0	-0.2	0.0			
							0.0	0.2	0.1			

FIG. 7. Visual extinction map of B 133 made from the blue-sensitive plate listed in Table I.

BARNARD 335

α_0 (1975) = $19^h\ 35^m\ 42.0^s$ δ_0 (1975) = $7°\ 31'\ 0.0''$

ℓ_{II} = 43.0 b_{II} = −7.0

STEWARD PLATE 616 PASSBAND CENTER = 7500 Å

RESEAU SCALE = 50.0″

								0.8	1.0	0.3				
								0.5	0.9	0.4				
								0.3	1.1	0.5				
			0.3	0.3	0.5	-0.0	0.7	0.1	0.6	0.5	0.3	0.8	0.6	0.6
			0.3	0.5	0.2	0.2	0.2	0.6	0.4	0.6	0.2	0.6	0.6	0.6
			0.3	0.2	0.7	0.5	0.6	1.2	1.1	1.1	-0.0	0.2	0.6	0.2
			0.2	-0.0	0.0	0.2	0.7	1.2	1.2	0.6	1.0	0.3	0.7	0.3
			0.0	0.6	0.9	1.1	2.0	2.2	1.0	0.3	0.6	1.2	0.2	0.3
0.3	0.3	0.1	0.2	0.6	0.8	7.4	7.4	3.1	1.5	1.1	0.1	0.2	0.6	0.0
0.3	0.6	0.1	-0.0	0.1	0.6	4.1	7.4	4.1	0.8	1.4	0.1	-0.1	0.1	0.4
0.8	0.5	-0.1	0.1	0.6	0.7	1.5	7.4	3.5	1.4	0.3	-0.2	0.2	0.5	0.5
			0.7	0.2	0.8	1.4	1.8	0.9	-0.0	0.3	-0.0	0.6	-0.0	-0.1
			0.3	0.2	-0.0	-0.2	0.0	0.2	-0.1	-0.1	0.4	0.2	0.1	0.1
			-0.2	0.3	-0.2	-0.0	0.3	-0.3	-0.1	-0.1	0.0	-0.1	-0.1	-0.1

FIG. 8. Visual extinction map of B 335 made from the far-red sensitive plate listed in Table I.

with radio observations made at 2.6-arcmin resolution, will further improve the concordance between extinctions obtained at two colors (cf. especially Table 1 in Dickman 1977).

It is a straightforward matter to determine minimum cloud masses from the maps of Figs. 6–13, if the distances to the sources are known and a standard gas to extinction ratio is utilized. One has for the cloud mass in terms of the visual extinction $A_V{}^i$ in each reseau element i:

$$M = (\alpha d)^2 (N_{H_2}/A_V)\mu \sum_i A_V{}^i. \qquad (12)$$

Here α is the reseau size in radians, d the distance to the cloud in centimeters, (N_{H_2}/A_V) the standard gas-to-extinction ratio $\sim 1.25 \times 10^{21}$ cm^{-2} mag^{-1} (Jenkins and Savage 1974), which assumes complete conversion of hydrogen in the cloud to molecular form, and μ the mean particle mass, which includes a $\sim$30% correction by weight for helium (Allen 1973). In the present work the summation was carried out only over reseau squares having $A_V{}^i \geq 0.5$ mag.

Results for the cloud masses are given in Table II. Distances are those given by Bok and McCarthy (1974). In the case of B 133 and B 335, the advantage of using red-sensitive plates to obtain a lower limit to the extinctions through the opaque cloud cores is evident. This is also true for B 92, where the double-core structure of the globule is resolved only in the red; unfortunately, the red-sensitive star counts clearly cover too small an area

BARNARD 335

α_0 (1975) = $19^h\ 35^m\ 42.0^s$ δ_0 (1975) = $7°\ 31'\ 0.0''$

ℓ_{II} = 43.0 b_{II} = −7.0

POS PLATE 0574 PASSBAND CENTER = 4280 Å

RESEAU SCALE = 66.7″

						0.2	0.2			
						0.0	0.2			
		0.1	0.1	0.3	0.1	0.5	0.2	0.0	-0.1	0.0
		0.2	0.5	0.2	0.4	0.1	0.1	0.2	-0.2	0.0
		0.1	-0.1	0.2	0.2	-0.0	0.3	0.1	-0.1	-0.1
		0.1	0.3	0.0	0.4	0.5	0.4	0.3	0.1	-0.0
		0.1	0.5	0.8	0.8	1.9	0.5	0.1	0.3	0.0
0.1	0.2	0.0	0.4	0.7	1.5	1.9	0.6	0.6	0.3	-0.1
-0.1	-0.1	0.6	1.1	1.7	3.4	2.3	1.1	0.3	0.3	-0.1
0.0	0.4	0.2	0.5	1.5	3.4	2.8	0.9	-0.1	0.1	0.0
0.1	0.1	0.4	0.5	1.7	2.8	1.5	0.3	-0.1	0.3	-0.1
		0.1	0.0	0.1	0.4	0.0	-0.0	-0.1	0.2	-0.2
		-0.1	-0.1	-0.2	-0.0	0.1	0.0	-0.2	-0.1	-0.2

FIG. 9. Visual extinction map of B 335 made from the blue-sensitive plate listed in Table I.

BARNARD 92

α_0 (1975) = $18^h\ 14^m\ 12.0^s$ δ_0 (1975) = $-18°\ 16'\ 0.0''$

ℓ_{II} = 12.7 b_{II} = −0.7

POS PLATE E810 PASSBAND CENTER = 6500 Å

RESEAU SCALE = 66.7″

				0.6	0.6						
				0.7	0.2						
				0.7	0.4						
				0.3	0.2						
				0.2	0.0						
				0.1	0.4						
0.6	0.6	1.0	0.2	0.7	0.9	0.8	0.6	0.8	1.8	0.8	0.0
0.4	0.4	0.6	0.4	0.2	0.6	0.4	1.4	0.6	0.3	0.9	0.4
				0.3	1.4	2.2	1.3	2.0	1.0	1.1	0.2
				1.0	3.3	5.5	3.3	1.2	0.9	1.0	0.6
				1.7	5.5	5.5	1.4	1.3	2.0	1.7	1.8
				3.3	4.1	3.3	1.8	1.1	0.8	0.7	0.5
0.6	0.8	0.7	1.5	2.8	3.3	2.8	0.8	1.3	1.1	1.0	0.4
0.5	0.6	0.5	0.8	5.0	4.1	4.1	1.3	1.7	1.1	0.8	0.7
0.8	0.6	0.2	0.1	5.0	2.2	1.7	2.2	1.0	1.4	0.8	0.9
			0.6	1.0	2.0	1.4	0.8	1.5	1.0	0.6	0.6
				1.4	2.8						
				1.0	1.4						
				0.2	0.4						
				0.4	0.6						
				0.3	0.4						
				0.3	0.3						

FIG. 10. Visual extinction map of B 92 made from the red-sensitive plate listed in Table I.

BARNARD 92

α_0 (1975) = $18^h\ 14^m\ 12.0^s$ δ_0 (1975) = $-18°\ 16'\ 0.0''$

ℓ_{II} = 12.7 b_{II} = −0.7

POS PLATE 0810 PASSBAND CENTER = 4280 Å

RESEAU SCALE = 66.7″

				0.4	0.9	0.6	0.5					
				0.8	0.8	0.3	0.6					
				0.1	0.4	0.7	0.2					
				0.1	0.4	0.4	0.5					
				0.0	0.6	0.2	0.2					
				0.5	0.3	1.0	0.7					
1.0	0.4	0.6	0.0	0.3	1.0	1.3	1.3	1.3	1.9	2.6	1.7	0.3
0.5	0.6	0.2	0.3	0.4	0.8	1.7	1.3	2.2	1.7	0.7	1.3	0.8
				0.1	0.7	1.7	5.1	1.9	1.9	1.5	1.3	0.3
				0.5	1.0	2.2	5.1	5.1	1.7	1.2	1.3	0.9
				0.7	1.0	5.1	5.1	2.6	1.7	2.6	2.2	1.9
				1.2	3.2	5.1	5.1	3.2	1.9	1.1	0.7	0.9
0.4	0.3	0.4	0.9	2.6	5.1	5.1	5.1	1.9	1.9	1.5	0.6	0.5
0.5	0.3	0.3	0.8	0.5	5.1	5.1	3.2	2.6	1.9	1.7	1.2	0.3
0.3	0.8	0.6	0.6	0.6	2.6	2.6	1.9	3.2	1.3	1.7	1.1	0.6
			0.3	0.4	1.1	2.6	3.2	1.7	1.9	1.9	1.1	1.0
			0.8	0.6	1.9	3.2	2.6	1.7	2.2			
				0.7	0.8	2.6	3.2	2.6	2.2			
				0.4	0.2	1.0	2.6	1.3	1.3			
				0.9	0.5	0.9	1.5					
				0.7	0.4	0.7	1.1					
				0.3	0.1	0.6	0.7					

FIG. 11. Visual extinction map of B 92 made from the blue-sensitive plate listed in Table I.

of the cloud to yield a meaningful lower limit to the globule mass. For B 134, the close agreement between the masses derived from the red and blue plates illustrates well the validity of the star count reduction procedures discussed in this work.

A comparison of the masses derived here with the dust masses obtained by Bok and McCarthy (1974) for the same clouds can be made if one assumes a gas-to-dust mass ratio ~100–200 for the purposes of evaluating the latter data. Mass values derived in this fashion are shown in the last column of Table II. Because the dust masses obtained by Bok and McCarthy were determined from

TABLE II. Cloud masses.

Object	Distance[a] (pc)	Mass ($M_\odot$) This work	Mass ($M_\odot$)[b] Bok and McCarthy (1974)
B 133 (B)	400	≥53	
B 133 (R)	400	≥59	~21–42
B 134 (B)	400	18	
B 134 (FR)	400	19	~1–2
B 335 (B)	400	≥14	
B 335 (FR)	400	≥23	~12–24
B 92 (B)	200	≥23	
B 92 (R)	200	≫9[c]	~8–16

[a] From Bok and McCarthy (1974).
[b] Gas-to-dust mass ratio ~100–200 assumed.
[c] Star counts did not cover a large part of cloud (cf. Figs 10 and 11).

BARNARD 134

α_0 (1975) = $19^h\ 5^m\ 36.0^s$ δ_0 (1975) = $-6°\ 17'\ 0.0''$

ℓ_{II} = 29.1 b_{II} = −6.3

POS PLATE 0692 PASSBAND CENTER - 4280 Å

RESEAU SCALE = 66.7″

					0.3	0.5	0.4	0.4	0.2	0.3							
					0.1	0.2	0.2	0.2	0.4	0.5							
					0.2	0.1	0.2	0.4	0.2	0.8							
					0.4	0.2	0.3	0.4	0.3	0.1							
			0.3	0.1	0.5	0.4	0.6	0.7	0.2	-0.0	-0.1	0.2	0.2				
			0.1	0.1	0.5	0.7	0.8	1.1	0.4	0.3	0.3	-0.1	0.0				
			0.1	0.2	0.9	2.8	1.4	0.1	0.3	0.1	0.1	0.1	0.1				
0.2	0.2	0.3	0.1	0.2	1.9	2.2	1.4	0.8	0.3	0.7	0.3	0.0	-0.2	-0.0	-0.0	0.0	0.1
-0.3	0.0	-0.1	0.1	0.8	2.8	2.8	1.1	1.4	0.8	0.4	0.5	0.2	0.2	0.2	0.3	0.1	0.[illegible]
0.3	0.1	-0.0	-0.0	0.4	2.8	2.8	2.8	1.1	1.4	0.6	0.8	0.2	0.5	0.1	0.1	0.2	-0.[illegible]
0.0	0.2	0.2	0.3	0.2	0.2	0.9	0.7	0.2	0.5	0.3	0.1	0.5	0.2	0.3	0.1	-0.1	0.[illegible]
			-0.1	-0.0	0.3	0.5	0.6	0.7	0.5	0.8							
			0.1	0.2	0.2	0.1	0.2	0.3	0.6	0.1							
					0.2	0.1	0.2	0.1									
					0.3	0.1	0.0	0.3									

FIG. 12. Visual extinction map of B 134 made from the blue-sensitive plate listed in Table I.

BARNARD 134

α_0 (1975) = $19^h\ 5^m\ 36.0^s$ δ_0 (1975) = $-6°\ 17'\ 0.0''$

ℓ_{II} = 29.1 b_{II} = -6.3

STEWARD PLATE 634 PASSBAND CENTER = 7500 Å

RESEAU SCALE = 50.0''

						0.8	0.1	0.4	0.6	0.1	0.3									
						0.2	0.8	0.4	0.6	0.2	0.2									
						0.4	0.6	0.4	0.2	0.4	0.2									
						1.0	0.6	0.1	0.5	0.8	0.3									
						0.1	0.1	0.7	1.1	0.4	-0.0									
			0.5	0.6	0.6	0.8	1.0	1.2	0.5	1.0	0.8	0.1								
			0.4	0.3	1.0	0.9	1.5	1.2	0.6	0.3	0.3	0.1								
			0.7	0.5	1.0	2.0	0.9	0.7	0.7	0.8	0.5	0.4								
			0.5	1.0	1.3	1.0	0.9	1.2	0.8	0.8	0.4	0.8								
0.2	0.2	-0.0	0.5	1.2	2.0	1.8	1.6	1.8	0.8	1.0	0.9	0.5	0.2	0.3	0.6	0.5	0.6	0.5	0.3	0.3
0.2	0.0	0.1	-0.1	0.9	1.3	2.1	2.9	2.0	2.0	1.4	0.7	0.4	0.5	0.9	0.3	0.5	0.0	0.4	0.7	0.7
-0.0	-0.3	0.1	0.9	0.1	0.6	2.0	1.4	1.0	0.7	0.9	1.1	0.5	0.5	1.0	0.2	0.8	0.2	0.5	0.6	0.6
			0.4	0.5	0.4	0.5	1.0	0.7	0.6	0.8	0.4	0.1								
			0.2	0.3	0.1	0.5	0.3	0.7	0.9	0.3	0.4	1.2								
			-0.2	0.1	-0.2	0.1	0.2	0.1	-0.0	0.2	0.6	0.5								
						0.6	-0.4	0.5												
						0.3	0.1	0.5												
						0.3	-0.2	0.1												

FIG. 13. Visual extinction map of B 134 made from the far-red sensitive plate listed in Table I.

measurements of the average extinctions for the clouds, the considerably higher mass limits obtained in the present work confirm the utility of making detailed extinction maps of dark nebulae in this context.

A treatment of the cloud masses and dimensions obtained here as they relate to the question of the gravitational stability of these globules is complex and lies beyond the scope of this paper. A detailed discussion of this subject, which includes data for several additional Bok globules whose masses were determined by the methods presented here is given elsewhere (Dickman 1978).

It is a pleasure to thank Professor B. J. Bok for providing access to the Steward Observatory plates used in this study, and for his enthusiastic instruction in the art of star counts. I also thank Dr. M. L. Kutner for several useful discussions. Work supported in part by NASA Grant NGR-33-008-191, National Science Foundation Grant MPS-73-04554, and The Aerospace Corporation's Company Programs for Research and Investigation.

APPENDIX: STATISTICAL ERRORS IN DERIVED VISUAL EXTINCTIONS

Combining Eqs. (5) and (10) one has for the visual extinction in a reseau square with n stars

$$A_V = \frac{K_{\lambda V}}{b_B}\log(n_0/n), \tag{A1}$$

where n_0 denotes the average number of reference field stars per reseau area, b_B is the slope of the van Rhijn sequence for the region of sky appropriate to the cloud, and $K_{\lambda V}$ is the factor transforming the extinction at the plate wavelength to its visual equivalent. Neglecting uncertainties in b_B and $K_{\lambda V}$, and noting that errors in n and n_0 are uncorrelated, the error in A_V is

$$\delta A_V = \frac{K_{\lambda V}}{b_B}\left[\left(\frac{\delta n}{n}\right)^2 + \left(\frac{\delta n_0}{n_0}\right)^2\right]^{1/2}, \tag{A2}$$

with a relative error

$$\frac{\delta A_V}{A_V} = \left[\log\left(\frac{n_0}{n}\right)\right]^{-1}\left[\left(\frac{\delta n}{n}\right)^2 + \left(\frac{\delta n_0}{n_0}\right)^2\right]^{1/2}. \tag{A3}$$

Here δn and δn_0 denote the uncertainties in the values of n and n_0, respectively; these are given by (Bok 1937)

$$\delta n = \sqrt{n}, \quad \delta n_0 = \sqrt{n_0}, \tag{A4}$$

if systematic counting biases are ignored or assumed uniform.

Accordingly, (A2) and (A3) become

$$\delta A_V = \frac{K_{\lambda V}}{b_B}\left(\frac{n + n_0}{n n_0}\right)^{1/2}, \tag{A5}$$

$$\delta A_V/A_V = \log\left(\frac{n_0}{n}\right)^{-1}\left(\frac{n + n_0}{n n_0}\right)^{1/2}. \tag{A6}$$

To estimate typical values for the above quantities, we note that for the red-sensitive star counts of B 133 made with a 50-arcsec reseau, $n_0 \simeq 48$, $b_B \simeq 0.42$, and $K_{\lambda V} \cong 1.2$. Thus, δA_V ranges from $\sim$0.58 mag at $A_V = 0$ (where $n = n_0$), to $\delta A_V \sim 2.89$ mag at $A_V \simeq 4.8$ (where $n = 1$ in a single reseau square). Correspondingly, the relative error (A6) is very large when $n \sim n_0$ (which accounts for the large scatter in Figs. 1–4 at low extinction values), and decreases to $\sim$0.6 for the case $n = 1$. Note that if (A5) and (A6) are to be applied to an opaque area in a cloud which is N reseau squares in extent, these relations should of course be evaluated with $n_0' = N n_0$ and $n = 1$.

REFERENCES

Allen, C. W. (1973). *Astrophysical Quantities* (Athlone, London).

Baker, P. L. (1976). Astron. Astrophys. **50,** 327.

Bless, R. C., and Savage, B. D. (1972). Astrophys. J. **171,** 293.

Bok, B. J. (1937). *The Distribution of Stars in Space* (Univ. Chicago P., Chicago).

Bok, B. J. (1948). Harvard Obs. Monogr. No. 7, p. 53.

Bok, B. J. (1956). Astron. J. **61,** 309.

Bok, B. J., and Cordwell, C. S. (1973). In *Molecules in the Galactic Environment,* edited by M. A. Gordon and L. E. Snyder (Wiley, New York), p. 53.

Bok, B. J., and McCarthy, C. C. (1974). Astron. J. **79,** 42.

Bok, B. J., Cordwell, C. S., and Cromwell, R. H. (1971). In *Dark Nebulae Globules and Protostars,* edited by B. T. Lynds (Univ. Arizona P., Tucson), Vol. 1, p. 37.

Carrasco, L., Strom, S. E., and Strom, K. M. (1973). Astrophys. J. **182,** 95.

Carrasco, L., Strom, K. M., and Strom, S. E. (1974). In *Planets, Stars, and Nebulae Studied with Photopolarimetry,* edited by T. Gehrels (Univ. Arizona P., Tucson), p. 954.

Dickman, R. L. (1976). Ph.D. dissertation, Columbia U.

Dickman, R. L. (1977). Astrophys. J. To be published.

Dickman, R. L. (1978). In preparation.

Encrenaz, P. J., Falgarone, E., and Lucas, R. (1975). Astron. Astrophys. **44,** 73.

Fitzgerald, M. P., Stephens, T. C., and Witt, A. N. (1976). Astrophys. J. **208,** 709.

Garrison, R. F. (1977). Bull. Am. Astron. Soc. **9,** 373.

Greenberg, J. M. (1968). In *Nebulae and Interstellar Matter,* edited by B. M. Middlehurst and L. H. Aller (Univ. Chicago P., Chicago), p. 221.

Harris, D. H. (1973). IAU Symp. No. 52, p. 3.

Hollenbach, D. J., Werner, M. W., and Salpeter, E. E. (1971). Astrophys. J. **163,** 165.

Jenkins, E. B., and Savage, B. D. (1974). Astrophys. J. **187,** 243.

Johnson, H. L. (1968). In *Nebulae and Interstellar Matter,* edited by B. M. Middlehurst and L. H. Aller (U. Chicago P., Chicago), Vol. 7, 167.

Kutner, M. L. (1973). In *Molecules in the Galactic Environment,* edited by M. A. Gordon and L. E. Snyder (Wiley, New York), p. 199.

Lilley, A. E. (1955). Astrophys. J. **121,** 559.

Lynds, B. T. (1962). Astrophys. J. Suppl. Ser. **7,** 1.

Myers, P. C. (1975). Astrophys. J. **198,** 331.

Rhijn, P. J. van (1929). Groningen Publ. **43**.

Schmidt, E. G. (1975). Mon. Not. R. Astron. Soc. **172,** 401.

Serkowski, K. (1973). IAU Symp. No. 52, p. 145.

Serkowski, K., Mathewson, D. S., and Ford, V. L. (1975). Astrophys. J. **196,** 261.

Sherwood, W. A. (1975). Astrophys. Space Sci. **34,** 1.

Strom, K. M., Strom, S. E., Carrasco, L., and Vrba, F. J. (1975). Astrophys. J. **196,** 489.

Trimble, V. (1977). Astrophys. Lett. **18,** 145.

Tucker, K. D., Dickman, R. L., Encrenaz, P. J., and Kutner, M. L. (1976). Astrophys. J. **210,** 679.

Vrba, F. J., Strom, K. M., Strom, S. E., and Grasdalen, G. L. (1975). Astrophys. J. **197,** 77.

Whitford, A. E. (1958). Astron. J. **63,** 201.

Wickramasinghe, N. C. (1972). In *Interstellar Matter,* edited by Astron. Inst. Univ. Basel (Geneva Obs., Sauverney), p. 207.